Available online at www.sciencedirect.com
SCIENCE DIRECT
Polymer 46 (2005) 3329–3336
polymer
www.elsevier.com/locate/polymer

Dye loading of unimolecular, amphiphilic polymeric nanocontainers

Michael Groß, Michael Maskos*

Institute of Physical Chemistry, University Mainz, Jakob-Welder-Weg 11, D-55099 Mainz, Germany

Received 1 September 2004; received in revised form 8 December 2004; accepted 7 February 2005
Available online 26 March 2005

Abstract

Unimolecular, amphiphilic polymeric nanocontainers based on poly(2-vinylpyridine)-*b*-polystyrene-polymacromonomers are dispersed in organic solvents and loaded with different hydrophilic dyes in solution. The poly-2-vinylpyridine core of the nanocontainers is responsible for the dye uptake, whereas the polystyrene corona grants the solubility and stabilization of the particles. The nanocontainers are 20–30 nm in diameter and possess an excellent ability to sequester dye molecules up to 116% (w/w) or 3.20 mmol/g.

Keywords: Nanoparticles; Amphiphilic; Macromonomers

1. Introduction

Due to the wide scope of potential applications, there has been an increasing interest in amphiphilic polymeric nanocontainers in recent times. Much of the research effort has been triggered by the search for new and more efficient drug delivery systems [1] and solubility enhancers [2]. Typical systems are block copolymer micelles [3], polyelectrolyte capsules [4], and liposomes [5]. One feature of these non-cross-linked systems is their-often desired-structural instability upon changes of the external condition, e.g. changes in the solvent quality or temperature. If structural integrity is intended, it is necessary to construct covalently fixed particles. Typical examples for amphiphilic core-shell nanoparticles are dendrimers [6], star-shaped block copolymers [7], cross-linked block copolymer micelles [8], and alkyl modified hyperbranched polyesters [9]. Another example is poly(organosiloxane) nanoparticles that can be prepared with defined core-shell structures with varying polarity [10]. Additional to the feature of structural integrity of those systems mentioned above, it is possible to introduce functionalities into the particles which would be incompatible with the non-cross-linked systems, e.g. they would prevent the particles from assembling. In cross-linked systems, the introduction of additional functionalities can be achieved after the formation of the particles [10].

Typical unimolecular nanocontainer systems like cross-linked blockcopolymer nanoparticles [11], hyperbranched polymers [12,13] or dendrimers [14,15] show maximum loading ratios of approximately 10% (w/w), one example up to 36% (0.70 mmol/g) [16].

In this work, we report on the synthesis of nanometer-sized polymeric particles with amphiphilic properties and demonstrate their excellent ability to solubilize, otherwise insoluble hydrophilic organic dye molecules in non-polar solvents. The covalently fixed particles are prepared by a free radical homopolymerization of end-functionalized block co-oligomers (block co-macromonomers) consisting of polystyrene (PS) and poly(2-vinylpyridine) (PVP), see Fig. 1 [17].

2. Experimental section

2.1. Materials

The solvents for purification purposes (benzene (Merck), low boiling petrol ether, 40/60 (Fisher Chemicals)) were refluxed over 0.1 wt% α,α'-azobisisobutyronitrile (Fluka, recrystallized from methanol) for 4 h before being distilled. 1-Nitropropane (p.a., Merck), dichloromethane (Acros) and ethanol (p.a., Merck) were used as received. Tetrahydrofurane (p.a., Riedel-deHaen) was dried over lithium aluminum hydride (Fluka). Styrene (Aldrich) and 2-vinyl pyridine (Acros) were dried over lithium aluminum hydride or

* Corresponding author. Tel.: +49 6131 3924 190; fax: +49 6131 3922 970.
E-mail address: maskos@mail.uni-mainz.de (M. Maskos).

0032-3861/$ - see front matter © 2005 Elsevier Ltd. All rights reserved.
doi:10.1016/j.polymer.2005.02.070

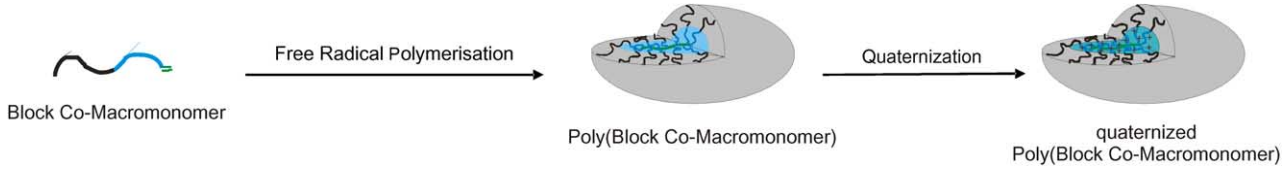

Fig. 1. Synthetic route for the preparation of amphiphilic core-shell nanoparticles.

calcium hydride (Aldrich), respectively. Ethylene oxide (Fluka), *sec*-butyl lithium (1.3 M solution in cyclohexane, Fluka) and bromomethane (Merck) were used as received. Water was purified with a Milli-Q deionizing system. The dyes calmagite and thymol blue, sodium salt (both Aldrich), methyl orange, sodium salt, ethyl orange, sodium salt and tropaeolin O, sodium salt (all Acros) were used as received.

2.2. Synthesis

Three different α-2-butyl-ω-(methacryloyloxy)polystyrene-*block*-poly(2-vinylpyridine) oligomers (block-co-macromonomers) with varying block length ratios and molecular weights have been synthesized by anionic polymerization techniques.[18] For a typical block-co-macromonomer synthesis, 6.9 mmol *sec*-butyl lithium (1.3 M solution in cyclohexane) were added to 500 mL tetrahydrofurane at −30 °C under argon. The solution was cooled to −75 °C and styrene monomer (312 mmol) was added dropwise. After 30 min, 2-vinyl pyridine (104 mmol) was added dropwise. A condenser is used for the addition of ethylene oxide and the temperature was slowly increased to room temperature. After 1 h, methacrylic acid chloride (10 mL) was added via syringe. Precipitation of the block-co-macromonomer in petrol ether yielded 95% of the crude product, which was purified by lyophilization from benzene. The core-shell nanoparticles with a non-polar shell consisting of polystyrene and a polar core of poly-2-vinylpyridine (poly(block co-macromonomer)) were obtained by free-radical polymerization of the block co-macromonomers.[19] Typically, 1 mL of a solution of AIBN in benzene (2 mg/mL) was added to 2 g block-co-macromonomer under argon and kept at 60 °C for 7 days. The solution was diluted with 10 mL benzene and the polymer was obtained by precipitation in petrol ether. Subsequent purification from the unreacted block co-macromonomer was performed by precipitation from benzene solution by slow addition of ethanol. Fig. 2 shows an example of this separation from unreacted macromonomer for $P(PS_{37}–PVP_9)_{164}$, as measured with SEC.

For the preparation of the quaternized polymer-brushes, in a typical experiment 1 g of the neutral polymer was dissolved in 1-nitropropane and 5 g of cooled bromomethane were added at −20°C. The reaction mixture was stirred at room temperature for one week. The product was isolated by precipitation in low-boiling petrol ether and finally freeze-dried from benzene.

2.3. Dye loading experiments

Polymer solutions were prepared with concentrations of $c_{Polymer} = 0.5$ g/L in different organic solvents. Typically, 2 mL of the polymer solutions were brought into contact with an excess of solid dye powder (5 mg) or 2 mL dye solution in Milli-Q water (concentrations $c = 2.5$ g/L). Phase transfer experiments were carried out in tightly sealed containers at room temperature in the dark without any stirring. After completion of the transfer, all phases were examined by UV/Vis spectroscopy. Colored solutions were diluted with pure solvent and/or freed from solid dye powder by filtration through Millipore Dimex-13 (0.2 μm) filters, if necessary.

2.4. Characterization

Proton NMR spectra in $CDCl_3$ were recorded on a Bruker AM-400 spectrometer operating at 400 MHz.

Size exclusion chromatography was performed on a system with a Waters 510 HPLC pump equipped with Styragel polymer columns (10^3, 10^4, 10^6 Å nominal pore diameter) in DMF (+1 g/L LiBr) at a flow rate of 1 mL/min at 60 °C and refractive index detection with a Waters 410 differential refractometer and a Water 486 UV-absorption detector operating at $\lambda = 275$ nm.

Matrix-assisted laser desorption ionization time-of-flight (MALDI-ToF) mass spectra were recorded with a Micromass TofSpec E in reflection mode. Samples have been

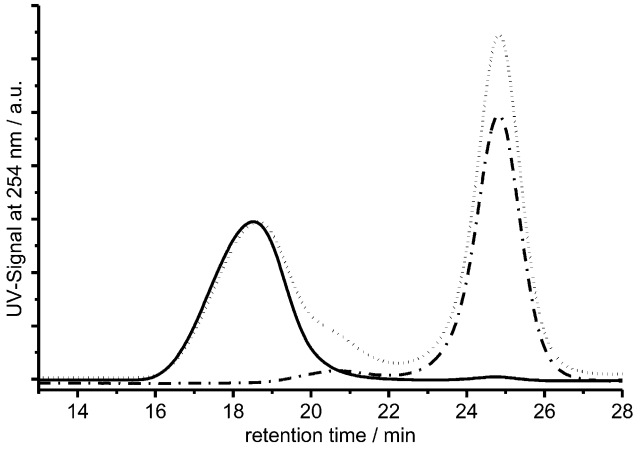

Fig. 2. SEC trace of $P(PS_{37}–PVP_9)_{164}$ (left peak) and the corresponding macromonomer (right peak). Dotted: reaction mixture before fractionation; dash-dotted: macromonomer and solid: polymacromonomer after fractionation. Solvent: DMF, 1 g/L LiBr.

prepared on a target using 1 μL of 5:5:2 mixed solutions of a 1 g/L solution of the polymer, 10 g/L 3-indoleacrylic acid (IAA) and silver trifluoroacetate, each in THF.

Static and dynamic light scattering was performed at 20 °C with an ALV SP-86 goniometer, a ALV/High QEAPD Avalanche photodiode fiber optic detection system, an ALV-3000 correlator, and a helium–neon laser (JDS Uniphase, $\lambda = 632.8$ nm, 25 mW). Measurements were carried out from 30 to 150° in 5 and 20° steps (static and dynamic measurements, respectively). Samples were prepared by dissolution in DMF (+1 g/L LiBr) and filtration using Millipore FG filters (0.2 μm) prior to the measurements. The refractive index increments were calculated according to $dn/dc = 0.165 m_{St} + 0.157 m_{PVP}$, with m_{St} and m_{PVP} being the mass fractions of styrene and poly-2-vinylpyridine of the block co-macromonomers, respectively.[20]

UV/Vis spectra were measured with a Cary 100 Bio spectrometer (Varian) employing 1 mm-quartz glass cuvettes (100-QS type, Hellma) from 300 to 700 nm.

3. Results and discussion

The synthesis of the nanocontainers involves two steps (Fig. 1). First, block co-macromonomers are prepared by an anionic polymerization technique, which provides an excellent control of the average molecular weights and the polydispersity of the oligomers. The second step is the free-radical polymerization of the block co-macromonomers to finally obtain the polymer comb in which each repeating unit of the methacrylate main-chain carries a poly(2-vinylpyridine)-*b*-polystyrene side-chain. The final product resembles a micellar structure, which is covalently fixed by the main-chain (unimolecular micelle). The overall shape of the polymer comb depends on the degree of polymerization of the main chain, which itself is influenced by the molecular weight of the macromonomer; in case of side-chain masses larger than approximately 4000 g/mol, more or less spherical structures are built, in case of lower molecular weights cylindrical nanoparticles can be obtained [21]. In both cases a core-shell topology is obtained. The non-polar shell of PS grants the solubility in organic solvents such as toluene or dichloromethane, while the core consists of polar PVP. In an additional step, the core's pyridine-units can be quaternized with e.g., methylbromide to obtain a polyelectrolyte with increased polarity compared to the neutral polymer.

By this synthetic route, polymeric core-shell nanoparticles with varying amounts of PVP with weight average molecular weights of 410 and 850 kg/mol and diameters of 20–30 nm have been obtained. Table 1 summarizes the characterization data.

As an example, the SEC trace of $P(PS_{37}–PVP_9)_{164}$ in DMF is shown in Fig. 2. The determined polydispersities of the samples are modest and range between 1.33 and 1.70. The characteristic ratio $\rho = R_g/R_h$ as obtained by static and

Table 1
Characterization data of the investigated polymers

Block co-macromonomers				Poly(block co-macromonomers)					Quaternized poly(block co-macromonomers)	
	M_n[a] (g/mol)	M_w/M_n	f[b] (%)	M_w[c] (g/mol)	R_g, app[c] (nm)	R_h, app[d] (nm)	P_w[e]	Purity[f] (%)	PDI[g]	f_{Quat}[h] (%)
$PS_{37}–PVP_9–MM$	4950	1.05	>60	$P(PS_{37}–PVP_9)_{164}$	8.5×10^5	17.8	15.1	164	98.5	1.65	$PQ–(PS_{37}–PVP_9)_{164}$	80
$PS_{38}–PVP_{11}–MM$	5280	1.04	>70	$P(PS_{38}–PVP_{11})_{138}$	7.6×10^5	15.3	14.3	138	99.5	1.70	$PQ–(PS_{38}–PVP_{11})_{138}$	70
$PS_{103}–PVP_7–MM$	12,100	1.05	>50	$P(PS_{103}–PVP_7)_{33}$	4.1×10^5	12.9	11.3	33	97.0	1.33	$PQ–(PS_{103}–PVP_7)_{33}$	70

Subscribed numbers in the polymers' names indicate the number average degree of polymerization of the corresponding block.
[a] MALDI ToF MS.
[b] Degree of functionalization, ^{1}H NMR.
[c] Static light scattering; solvent: DMF+LiBr (1 g/L).
[d] Dynamic Light Scattering; solvent: DMF+LiBr (1 g/L).
[e] Degree of polymerization of main chain.
[f] Weight ratio of block comacromonomer, determined by SEC; solvent: DMF+LiBr (1 g/L); rest: macromonomer.
[g] Polydispersity obtained by SEC; solvent: DMF+LiBr (1 g/L), calibrated with linear poly(2-vinylpyridine) standards.
[h] Degree of quaternization determined by elemental analysis; quaternized with methylbromide.

dynamic light scattering measurements ranges between 1.07 and 1.18. This leads to the conclusion that the nanoparticles have an ellipsoidal shape in solution. The nanoparticles were visualized by atomic force microscopy. As examples, $P(PS_{37}–PVP_9)_{164}$ and $PQ–(PS_{37}–PVP_9)_{164}$ are shown in Fig. 3a and b, confirming the average size and shape determined by light scattering.

In the present study, the polymer-assisted phase transfer of hydrophilic molecules into organic solvents is investigated. Several hydrophilic dyes are being used as models (Fig. 4), since they are available in a large variety (chemical structure, charge, etc.) and the transfer process is easily monitored, qualitatively even with the bare eye, quantitatively by UV/Vis spectroscopy.

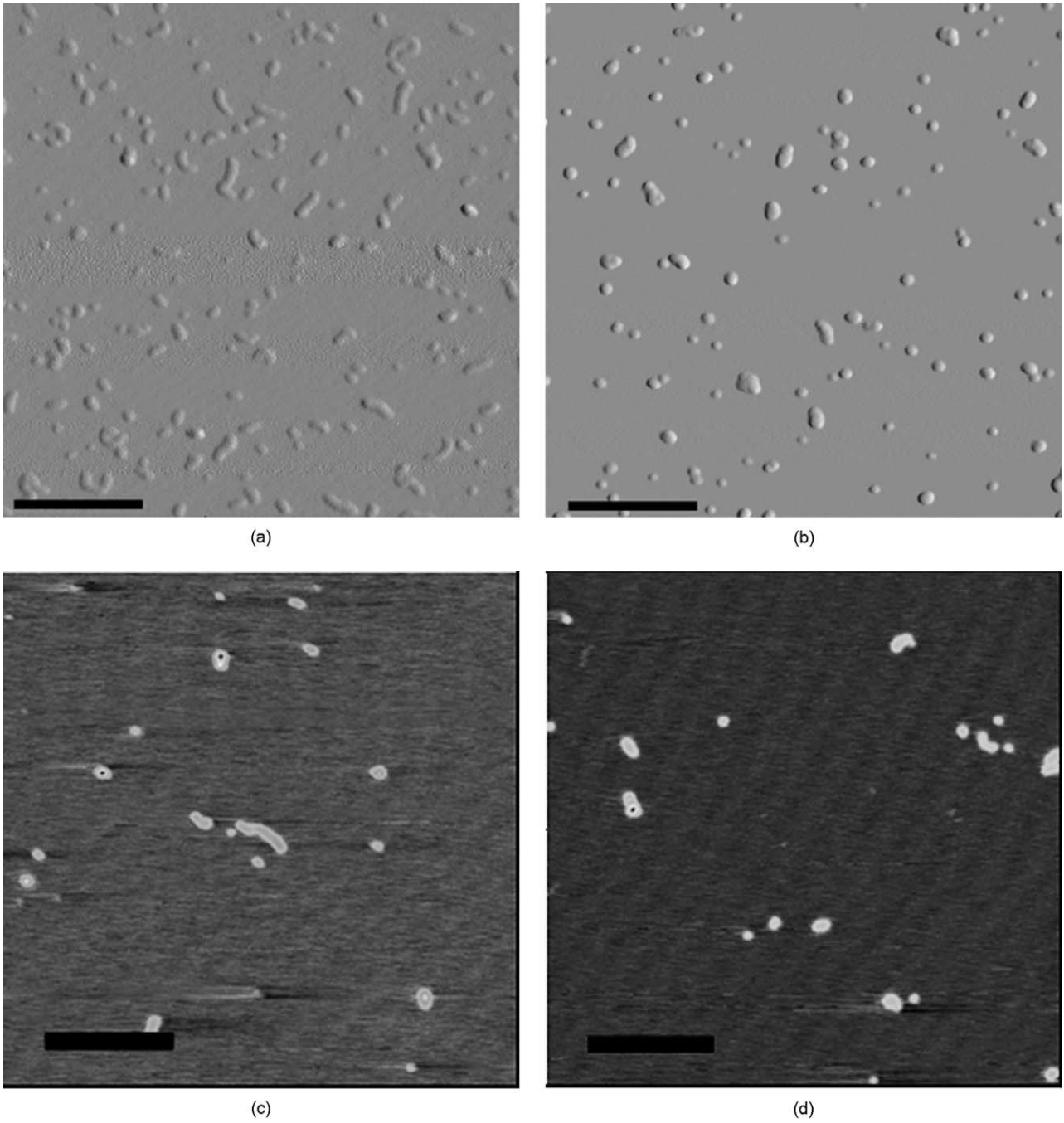

Fig. 3. (a) AFM picture (amplitude) of $P(PS_{37}–PVP_9)_{164}$, spin-cast onto mica from a 1:2 mixture of dichloromethane and cyclopentane ($c=0.166$ g/L). Scale bar: 250 nm. Average diameter $D=24.6$ nm. (b) AFM picture (amplitude) of $PQ–(PS_{37}–PVP_9)_{164}$, spin-cast onto mica from a 1:2 mixture of dichloromethane and cyclopentane ($c=0.033$ g/L). Scale bar: 250 nm. Average diameter $D=25.3$ nm. (c) AFM picture (height) of $P(PS_{38}–PVP_{11})_{138}$, loaded with Calmagite, spin-cast onto mica from a 1:2 mixture of dichloromethane and cyclopentane ($c=0.033$ g/L). Scale bar: 250 nm. Average diameter $D=31.8$ nm. (d) AFM picture (height) of $PQ–(PS_{38}–PVP_{11})_{138}$, loaded with Calmagite, spin-cast onto mica from a 1:2 mixture of dichloromethane and cyclopentane ($c=0.033$ g/L). Scale bar: 250 nm. Average diameter $D=33.1$ nm.

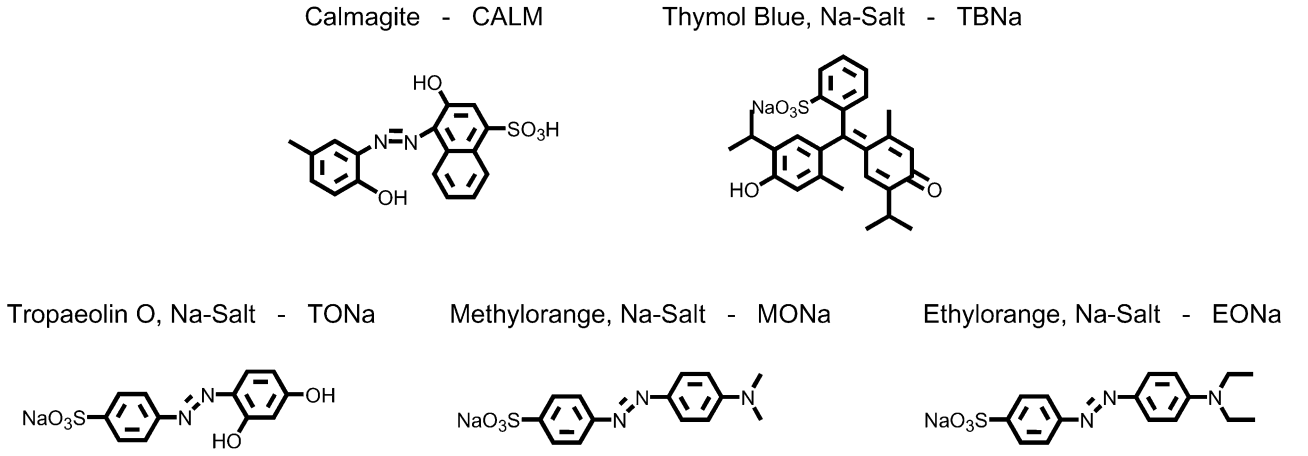

Fig. 4. Overview of the employed dyes.

Fig. 5 illustrates the two different routes to transfer hydrophilic molecules into non-polar organic solvents. Fig. 5a shows the solid/liquid phase transfer. An organic solution of the polymer is simply brought into contact with the solid dye powder.

Depending on the dye and polymer used, a coloration of the organic phase is observed almost instantly, indicating a successful transfer of the hydrophilic dye molecules. Without any agitation of the solution, the phase transfer is complete after 72 h, i.e. the absorption of the organic phase does not increase any further. An example of the solid/liquid phase transfer experiment is presented in Fig. 6a.

Fig. 5b depicts the second possibility to transfer hydrophilic molecules into the organic solvent by liquid/liquid phase transfer. Here, the organic solution of the polymer is brought into contact with an aqueous solution of the dye. The dye is removed from the water phase and transferred into the non-polar solvent by the polymer as seen for example in Fig. 6b.

The decrease of the dye concentration in the water phase is monitored quantitatively by UV/Vis spectroscopy and this depletion, as determined by λ_{max}, is related to the amount of dye transferred into the polymeric nanoparticles under the assumption of absence of precipitation of the dye or the polymer at the interface. Absorption measurements of the organic phase yield only relative values, because the dye itself is not soluble in the non-polar solvent and no calibration according to Lambert-Beer's law is obtainable. The corresponding data obtained at λ_{max} are summarized in Table 2.

Probably the most dominant factor that promotes the phase transfer is the interaction of the dye with poly(2-vinylpyridine). Linear oligomeric PVP, which is reasonably soluble in, e.g. toluene, dissolves the hydrophilic dye, whereas polystyrene does not support a phase transfer of hydrophilic dyes into organic solvents (data not shown). Thus the relative amount of PVP influences the maximum dye uptake by the polymer, whereas PS grants the solubility of the nanoparticles.

Quantitative investigation of the dye uptake by liquid/liquid phase transfer yields the number ratios n_{Dye}/n_N, where the number of dye molecules is related to the number of pyridine units or pyridinium units in the neutral or quaternized polymers, respectively.

The mass ratio $m_{Dye}/m_{Polymer}$ is of interest with respect to potential applications. High ratios mean that a large amount of the desired polar molecules is made soluble (or compatible with a matrix) with the help of small amounts of encapsulating agent.

Additionally, Table 3 shows the number ratio $n_{Dye}/n_{Particle}$, emphasizing the high dye uptake capacities of the presented polymeric nanoparticles.

Some general observations are made when comparing the liquid/liquid with the solid/liquid phase transfer. The former is more effective, i.e. the dye uptake is higher, when one compares the absorbance of the organic phase (see Table 2).

Water obviously promotes the transfer process as can be seen from Table 2, but it is not necessarily required. Even when all substances are thoroughly dried and handled in an

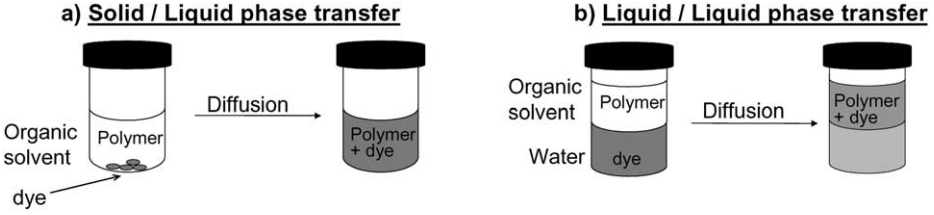

Fig. 5. Phase transfer experiments for the incorporation of hydrophilic dyes into polymeric particles.

Fig. 6. (a) Picture of a solid/liquid phase transfer experiment: Shown are the results of the phase transfer for EONa into dichloromethane. No addition of polymer (left) yields no transfer of the dye into the organic solvent, the neutral polymer $P(PS_{37}–PVP_9)_{164}$ (middle) is more effective than the quaternized $PQ–(PS_{37}–PVP_9)_{164}$ (right). (b) Picture of a liquid/liquid phase transfer experiment: Shown are the results of the phase transfer for Calmagite into toluene (upper layer). No addition of polymer (left) yields no transfer of the dye into the organic phase, the neutral polymer $P(PS_{103}–PVP_7)_{33}$ (middle) and the quaternized polymer $PQ–(PS_{103}–PVP_7)_{33}$ (right) are almost equally effective in the phase transfer.

inert atmosphere, a phase transfer of the dye into the non-polar solvent takes place and almost comparable uptakes are observed (data not shown), as compared to the solid/liquid phase transfer experiments with solvents and dyes employed as received and as discussed above. In most cases, higher dye uptakes are achieved by the liquid/liquid phase transfer.

When sodium salts of the dyes are used (TBNa, MONa, EONa, TONa) a strong influence of the polymer's charge is evident. The cationic polyelectrolyte can interact with the anionic dye molecules and a counterion exchange can take place. From quantitative measurements no complete ion exchange (number of anionic dye molecules vs. number of

Table 2
Comparison of solid/liquid phase transfer (S/L) and liquid/liquid phase transfer (L/L).

		CALM[a]		TBNa[b]		MONa[c]		EONa[d]		TONa[e]	
		S/L[f]	L/L[g]	S/L[f]	L/L[g]	S/L[f]	L/L[g]	S/L[f]	L/L[g]	S/L[f]	L/L[g]
$P(PS_{37}–PVP_9)_{164}$	DCM[h]	0.948	1.122	0.413	<0.01	0.234	0.242	0.983	0.670	0.292	0.307
$PQ–(PS_{37}–PVP_9)_{164}$	DCM[h]	0.501	1.049	0.617	0.526	0.109	1.096	0.429	1.327	0.059	0.758
$P(PS_{103}–PVP_7)_{33}$	DCM[h]	0.423	0.494	0.045	<0.01	<0.01	0.015	0.181	0.033	0.018	0.029
$PQ–(PS_{103}–PVP_7)_{33}$	DCM[h]	0.282	0.407	0.296	0.248	0.171	0.461	0.214	0.546	0.020	0.314
$P(PS_{103}–PVP_7)_{33}$	Tol[i]	0.231	0.401	0.043	<0.01	<0.01	<0.01	0.088	0.038	<0.01	0.010
$PQ–(PS_{103}–PVP_7)_{33}$	Tol[i]	0.123	0.385	0.209	0.134	<0.01	0.371	0.050	0.444	0.020	0.024

Table lists the absorption (λ_{max}) of the organic phase after phase transfer. Initial polymer concentration is $c_{Polymer}=0.5$ g/L.

[a] Calmagite.
[b] Thymol Blue, sodium salt.
[c] Methyl Orange, sodium salt.
[d] Ethyl Orange, sodium salt.
[e] Tropaeolin O, sodium salt.
[f] Solid/liquid phase transfer.
[g] Liquid/liquid phase transfer.
[h] Dichloromethane.
[i] Toluene.

Table 3
Dye loading capacities of different polymers via liquid/liquid phase transfer for several dyes

		CALM[a]			TBNa[b]			MONa[c]			EONa[d]		
		m_D/m_P[e]	n_D/n_N[f]	n_D/n_{Part}[g]	m_D/m_P[e]	n_D/n_N[f]	n_D/n_{Part}[g]	m_D/m_P[e]	n_D/n_N[f]	n_D/n_{Part}[g]	m_D/m_P[e]	n_D/n_N[f]	n_D/n_{Part}[g]
$P(PS_{37}–PVP_9)_{164}$	DCM[h]	116	1.78	1586	1	0.01	9	11	0.18	160	14	0.22	196
$PQ–(PS_{37}–PVP_9)_{164}$	DCM[h]	104	1.82	1622	40	0.51	454	34	0.65	579	30	0.53	472
$P(PS_{103}–PVP_7)_{33}$	DCM[h]	51	2.40	420	9	0.30	53	5	0.27	47	3	0.12	21
$PQ–(PS_{103}–PVP_7)_{33}$	DCM[h]	52	2.50	438	21	0.74	130	16	0.87	152	12	0.58	102
$P(PS_{103}–PVP_7)_{33}$	Tol[i]	38	1.80	315	19	0.66	116	1	0.03	5	1	0.02	4
$PQ–(PS_{103}–PVP_7)_{33}$	Tol[i]	37	1.77	310	21	0.74	130	13	0.68	119	11	0.55	96

Given are the mass loading ratios $m_{Dye}/m_{Polymer}$ in percent and the number ratios n_{Dye}/n_N of dye molecules per pyridine/pyridinium unit in the polymer.
[a] Calmagite.
[b] Thymol blue, sodium salt.
[c] Methyl orange, sodium salt.
[d] Ethyl orange, sodium salt.
[e] Mass loading ratio $m_{Dye}/m_{Polymer}$ in percent.
[f] Number of dye molecules per pyridine/pyridinium unit in the polymer.
[g] Number of dye molecules per particle $n_{Dye}/n_{Particle}$.
[h] Dichloromethane.
[i] Toluene.

cationic pyridinium units of the polymer) is achieved in liquid/liquid phase transfer, as can be seen in Table 3.

For the azo-dyes methyl orange, ethyl orange and tropaeolin O, the general trend is observed that there is a strong increase in transfer capacity of the polymer, if its core (PVP) is quaternized and if the transfer takes place across the water/organic solvent layer interface (i.e. liquid/liquid phase transfer), as seen in Table 2. The first is attributed to the specific interaction between ions of dislike charge (anionic dye, cationic polymer), while the presence of water promotes the phase transfer for these dyes and is linked to the latter observation. In addition, the PVP-core of the neutral polymer should form the same kind of microenvironment in both transfer types (water is a poor solvent for neutral PVP and thus is probably not incorporated significantly into the particle's core), and consequently the dye loading ratios are comparable for both kind of phase transfers (Table 2). In contrast, water is a solvent for the quaternized PVP-core and is also transferred into the polyelectrolyte in the liquid/liquid phase transfer [22], creating a more 'dye friendly'-microenvironment, thus enhancing the loading capacity of the polymer. If water is missing, as in the solid/liquid phase transfer, a lower dye uptake by the quaternized PVP is observed (Table 2).

Interestingly, the triphenylmethane dye thymol blue is also incorporated better into the quaternized PVP-core (Table 2), but in this case water does not promote the phase transfer. This leads to the conclusion that water and the polarity of the dye have a strong influence on the phase equilibrium and the dye uptake by the nanoparticles. The complex details of the water uptake by the nanoparticles in liquid/liquid phase transfer are currently being investigated.

A special behavior is observed for the sulfonic acid calmagite. In solid/liquid phase transfer, the neutral polymer is clearly favored, which could be explained by protonation of the pyridine-units of the nanoparticle's core and subsequent specific ionic interaction. In liquid/liquid phase transfer, this effect is not as evident. It is obvious that pure specific ionic interaction cannot be the sole factor for the dye loading ratios and that additional interactions between the hydrophilic dye and the polymer, as for example the polarity of the microenvironment or hydrophobic interactions, may play a role especially for calmagite. The dye loading ratios (n_{Dye}/n_N) are all larger than 1.75 and thus very high numbers of dye molecules per particle are observed. This makes calmagite an interesting candidate for future investigations of the transfer kinetics and the transfer mechanism. AFM pictures of $P(PS_{38}–PVP_{11})_{138}$ and $PQ–(PS_{38}–PVP_{11})_{138}$, both loaded with calmagite by liquid/liquid phase transfer using dichloromethane as solvent, are shown in Fig. 3c and d, respectively. The loading capacities are determined to $m_{Dye}/m_P = 100\%$, $n_{Dye}/n_N = 1.34$ and $n_{Dye}/n_{Part} = 1194$ for $P(PS_{38}–PVP_{11})_{138}$ and $m_{Dye}/m_P = 80\%$, $n_{Dye}/n_N = 1.22$ and $n_{Dye}/n_{Part} = 1087$ for $PQ–(PS_{38}–PVP_{11})_{138}$. The average diameters of the nanoparticles on the surface are 31.8 and 33.1 nm, respectively. In addition,

dynamic light scattering of the calmagite filled nanoparticles $P(PS_{38}–PVP_{11})_{138}$ was performed in toluene solution. Due to the fact that all employed dyes still possess substantial absorption at the wavelength of the laser of 632.8 nm, the data have to be treated carefully. Nevertheless, in this case an apparent hydrodynamic radius $R_h = 16.4$ nm was determined, in good agreement with an increase in radius as compared to the unloaded nanoparticles.

The influence of the organic solvent used in the transfer experiments is quite obvious. In both solid/liquid and liquid/liquid phase transfer, dichloromethane is the better choice compared to toluene for achieving higher loading ratios. This is understood, because dichloromethane has the larger dielectric constant and promotes the phase transfer. In addition, the solubility of the core's PVP in this solvent is better, making it easier accessible for the dye molecules.

The influence of the polymer's side chain composition on the dye uptake capability of the nanoparticles can be seen from the comparison of the n_{Dye}/n_N ratios for $P(PS_{37}–PVP_9)_{164}$ and $P(PS_{103}–PVP_7)_{33}$ (and their quaternized counterparts) from Table 3. It is evident that the particles with the larger PS blocks in the side chains can complex more dye molecules in their poly(2-vinylpyridine) cores. A reasonable explanation for this observation is the fact that the longer PS corona hinders the diffusion of the dye back into the less favorable solvent more effectively. The mass loading ratios $m_{Dye}/m_{Polymer}$ also indicate that PS affects the dye loading only indirectly and that PS is not responsible for the interaction with the polar molecules.

4. Conclusion

We have shown that it is possible to synthesize versatile polymeric core-shell nano-containers with high loading capacities for hydrophilic molecules by a macromonomer approach. The structures of these particles resemble unimolecular micelles that keep their integrity even upon isolation and dissolution in non-selective solvents. Hydrophilic dyes were incorporated into the polymeric particles via solid/liquid or liquid/liquid phase transfer, respectively. The quantification of the dye uptake is possible for the liquid/liquid phase transfer and yields mass loading ratios up to 116% (3.20 mmol/g). These high loading capacities, especially in case of calmagite, might be explained by the 'perfect' microenvironment provided by the nano-containers and the comparably 'open' structure of the polymer combs. After the incorporation of the otherwise insoluble dyes, the dye-polymer conjugates can be isolated from solution and are fully redisperisable in organic solvents.

Acknowledgements

We would like to thank Prof. Manfred Schmidt for the fruitful discussions and the BASF AG, Germany, for financial support.

References

[1] Uhrich KE, Cannizzaro SM, Langer RS, Shakesheff KM. Chem Rev 1999;99:3181.
[2] Horn D, Rieger J. Angew Chem 2001;113:4460.
[3] (a) Allen C, Han J, Yu Y, Maysinger D, Eisenberg A. J Control Release 2000;63:275.
(b) Allen C, Eisenberg A, Mrsic J, Maysinger D. Drug Delivery 2000; 7:139.
(c) Riegel IC, Samios D, Petzhold CL, Eisenberg A. Polymer 2003; 44:2117.
(d) Choucair A, Lavigueur C, Eisenberg A. Langmuir 2004;20:3894.
[4] (a) Shi XY, Caruso F. Langmuir 2001;17:2036.
(b) Tiourina OP, Antipov AA, Sukhorukov GB, Larinova NL, Möhwald H. Macromol. Biosci. 2001;1:209.
[5] Leonetti C, Biroccio A, Benassi B, Stringaro A, Stoppacciaro A, Semple SC, Zupi G. Cancer Gene Ther 2001;8:459.
[6] (a) Jansen JFGA, de Brabander-van der Berg EMM, Meijer EW. Science 1994;266:1226.
(b) Manna A, Imae T, Aoi K, Okada M, Yogo T. Chem Mater 2001; 13:1674.
[7] Pistel KF, Bittner B, Koll H, Winter G, Kissel T. J Controlled Release 1999;59:309.
[8] Shchukin DG, Sukhorukov GB. Adv Mater 2004;16:671.
[9] Schmaljohann D, Pötschke P, Hässler R, Voit BI, Froehling PE, Mostert B, Loontjens JA. Macromolecules 1999;32:6333.
[10] Jungmann N, Schmidt M, Ebenhoch J, Weis J, Maskos M. Angew Chem Int Ed 2003;42:1714.
[11] Ding J, Liu G. J Phys Chem B 1998;102:6107.
[12] Schmaljohann D, Pötschke P, Hässler R, Voit BI, Fröhling PE, Mostert B, Loontjens JA. Macromolecules 1999;32:6333.
[13] Stiriba S-E, Kautz H, Frey H. J Am Chem Soc 2002;124:9698.
[14] Dykes GM, Brierley LJ, Smith DK, McGrail PT, Seeley GJ. Chem Eur J 2001;7:4730.
[15] Arkas M, Tsioirvas D, Paleos CM. Chem Mater 2003;15:2844.
[16] Ghosh SK, Kawaguchi S, Jinbo Y, Izumi Y, Yamaguchi K, Taniguchi T, Nagai K, Koyama K. Macromolecules 2003;36:9162.
[17] (a) Tsukahara Y, Mizuno K, Segawa A, Yamashita Y. Macromolecules 1989;22:1546.
(b) Tsukahara Y, Tsutsumi K, Yamashita Y, Shimada S. Macromolecules 1990;23:5201.
[18] Djalali R, Hugenberg N, Fischer K, Schmidt M. Macromol Rapid Commun 1999;20:444.
[19] Dziezok P, Sheiko SS, Fischer K, Schmidt M, Möller M. Angew Chem 1997;109:2894.
[20] Djalali R. Dissertation, University of Mainz, Germany; 2002.
[21] Wintermantel M, Gerle M, Fischer K, Schmidt M, Wataoka I, Urakawa H, Kajiwara K, Tsukahara Y. Macromolecules 1996;29:978.
[22] Khougaz K, Gao Z, Eisenberg A. Langmuir 1997;13:623.